J. Materials, Conc. Struct. Pavements, JSCE, No. 690/V-53, 159-174, 2001 November

SHEAR FAILURE OF RC MEMBERS SUBJECTED TO PRE-CRACKS AND COMBINED AXIAL TENSION AND SHEAR

Amorn PIMANMAS[1] and Koichi MAEKAWA[2]

[1] Member of JSCE, Ph.D., Research fellow, Dept. of Civil Eng., The University of Tokyo
(Hongo 7-3-1, Bunkyo-ku, Tokyo 113, Japan)
[2]Member of JSCE, Dr. of Eng., Professor, Dept. of Civil Eng., The University of Tokyo
(Hongo 7-3-1, Bunkyo-ku, Tokyo 113, Japan)

The effect of loading path on the behavior of RC members is investigated. The shear capacity of RC members under coupled axial tension-shear is discussed. Three main effects of axial tension are (1) early yielding of main bar due to initial stress; (2) axial tensile stress accelerates the formation of diagonal crack and (3) pre-cracks caused by axial tension blunt the localization of diagonal cracks. The increase or decrease in shear capacity is possible depending on the relative effect of these three factors. JSCE design code seems to recognize only the first factor without explicit coverage of the second and the third ones. Comparative study of experimental results, JSCE and FEM predictions is conducted.

Key Words: *pre-cracked RC, non-proportional loading path, failure envelope, path-dependency, coupled axial tension/shear*

1. INTRODUCTION

Any RC members, pre-cracked or initially un-cracked members may be subjected to the generic multi-directional non-proportional loading paths during its life (**Fig.1**). Moreover RC members may be exposed to the past loading and environmental attack, which generate cracks inside them. These pre-cracks generally have a variety of width and inclination. Recent experiments on pre-cracked beams by the authors lead to the rational insight into the effect of these pre-cracks[1),2)].

Numerical analysis based upon FEM is conducted to simulate the shear response of pre-cracked RC members[2),3)]. The influence of the width, the inclination of pre-crack as well as the interaction with neighboring cracks can be simulated. The capability of FEM is rooted in the fact that it can reproduce mechanics of pre-cracked element[1)-4)], which is rooted in the shear anisotropy along the pre-crack plane.

In addition to pre-cracks, previous loading and environmental attacks may concurrently induce the state of pre-stress inside RC members. For example, it is known that concrete at an early age may be subjected to drying and autogeneous shrinkage as well as thermal heat attack[5)]. These mechanisms,

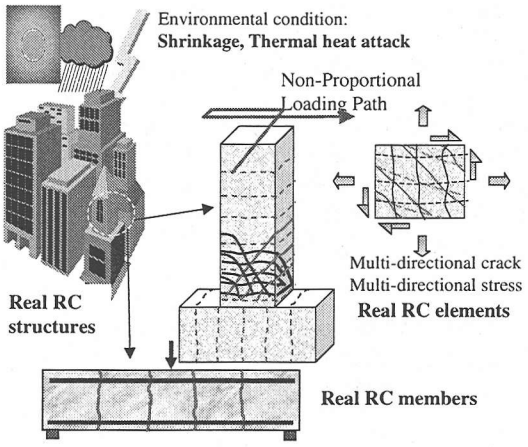

Fig.1 Real RC structures, members and elements subjected coupled generic loading paths and real environment

not only induce cracks but also result in the state of residual or pre-stress to concrete members. Hence, it is necessary to discuss the coupled effect of pre-stressed and pre-cracked state on the RC behavior.

Moreover, RC members may be subjected to a generic non-proportional loading path. Concrete is a highly path-dependent material that memorizes the past cracking events. Consequently, the behavior of RC member cannot be sufficiently defined by only the starting and ending points of the loading path,

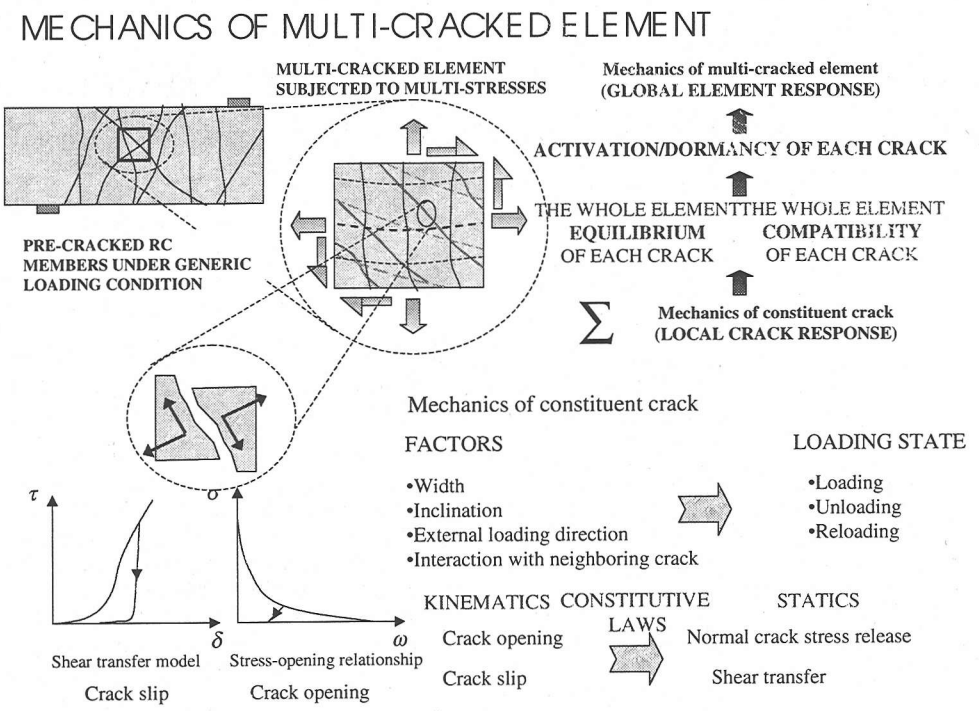

Fig.2 Mechanics of multi-cracked element subjected multi-stress state

but must be described also by the paths through which the member has experienced.

Therefore, even if two identical reinforced concrete members start from the same initial point and reach another same ending point, the response may be different if they undergo different loading paths. The paper aims at investigating the influence of the loading path on RC member by analyzing the RC member under combined axial tension-shear, and pre-cracked conditions.

2. MECHANICS OF MULTI-CRACKED RC ELEMENT AND SHEAR ANISOTROPY

In order to achieve the numerical simulation of the aforementioned problem, the analytical method must be able to capture the mechanics of multi-cracked element subjected to a multi-directional stress state. The mechanics of a multi-cracked element is illustrated in **Fig.2**. The overall response of a multi-cracked element under a multi-directional stress condition is assembled from local crack responses of all cracks in the element. The compatibility and equilibrium conditions of each crack in the element and the un-cracked concrete must be simultaneously satisfied.

The behavior of each constituent crack depends on its width, the inclination, the external loading, magnitude and direction, and the interaction with neighboring cracks. The interaction is described by the fact that the loading condition of one crack may subject other cracks to the loading or unloading or reloading conditions depending on their geometrical and physical properties.

The loading conditions, i.e., loading, unloading or reloading, of each crack must satisfy the equilibrium and compatibility in the local crack direction. This is the requirement of the equilibrium and compatibility of the RC element that constitutes the whole member. Through the simultaneous satisfaction of equilibrium and compatibility of all cracks in the element, certain cracks can be activated whereas others are idle. This results in crack interaction, which is classified as a special case of ***Anisotropy interaction*** as shown in **Fig. 3**.

Under a multi-cracking condition (**Fig.3, left**), the activation of some cracks dominates the overall behavior while other cracks are dormant. Under a uni-cracking condition (**Fig.3, right**), the activation of pre-crack relaxes the stress concentration in the diagonal direction, which affects the initiation of a new crack. Generally, the anisotropy interaction governs the local activation or dormancy of each crack in the element. Eventually, the spatial variation of crack activation/dormancy in each element over the whole domain governs the whole

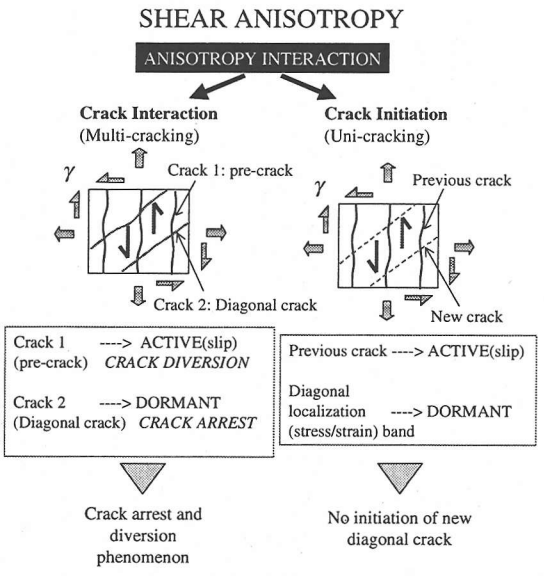

Fig.3 Shear anisotropy and anisotropy interaction

member or structural behavior. In order to simulate the shear anisotropy and crack interaction, the mechanics of local crack response is indispensable in the finite element analysis. Kinematics of crack is composed of crack opening and slip. Corresponding static variables are normal crack stress release and shear transfer stress, respectively. The constitutive laws are necessary to relate the kinematics and static variables together. These laws include tension stiffening/bridging softening and shear transfer due to aggregate interlock, respectively.

3. FOUR-WAY FIXED CRACK MODEL

In order to deal with the non-proportional loading path and multi-cracking situation, the fixed crack scheme and the active crack strategy are indispensable to capture the crack interaction. The fixed crack model considers both Mode I tensile stress release and Mode II shear transfer, therefore it allows the independent and explicit treatment of shear and normal behaviors. This is the basic requirement of anisotropy since principal stress vector does not necessarily coincide with that of principal strain. Moreover, the fixed crack approach records the crack condition and other state variables at all Gauss points, which allows the transfer of path-dependency over loading stages.

One of the recent developments in line with the fixed crack approach is the four-way fixed crack model proposed by Fukuura and Maekawa[6),7)]. This crack model can cover up to four cracks in distinct orientations at any Gauss point (**Fig.4**).

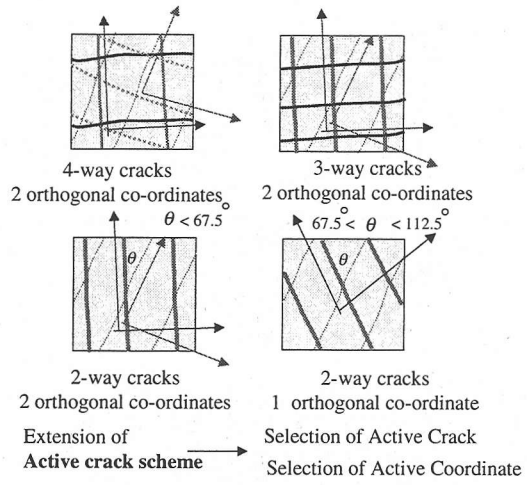

Fig.4 Coverage of four-way fixed crack approach[6),7)]

The active crack hypothesis[8)] is still preserved but the applicability has been extended into the co-ordinate level. The stress computation is carried out along the active crack in the active co-ordinate. The crack with larger width is considered to be the active one[6)-8)].

Local constitutive laws are needed for computing stresses of concrete and reinforcing bars. The coupled tension-compression model, which combines the tension stiffening/softening[8),9)] and elasto-plastic fracture model[8)], is applied to compute the normal stresses perpendicular and parallel to the crack, respectively. The contact density model[10)] is used to compute the shear transfer due to aggregate interlock under the multi-cracking situation[6),7)]. The model for reinforcing bars considers the effect of localized plasticity[11)] at crack vicinities and the anisotropic tension stiffening/softening[12)]. These local constitutive laws were reformulated and detailed by Fukuura and Maekawa[6),7)].

4. ANALYSIS OF PRE-CRACKED BEAM : EFFECT OF PRE-CRACKS

The shear behavior of pre-cracked beam is analytically and experimentally investigated[1)-3)]. Experimental program is outlined in **Fig.5**. Penetrating pre-cracks were introduced into the beam by means of reversed flexural loading (**Fig.5a**). This required two steps of flexural loading. After the first flexure, the beam was rotated through 180°, then the second flexure was applied. To conduct shear test, supports were moved towards beam mid-span (**Fig.5b**) such that the shear span to effective depth ratio was 2.41. Reinforcement ratio of main bar was 1.14%. Tested average compressive

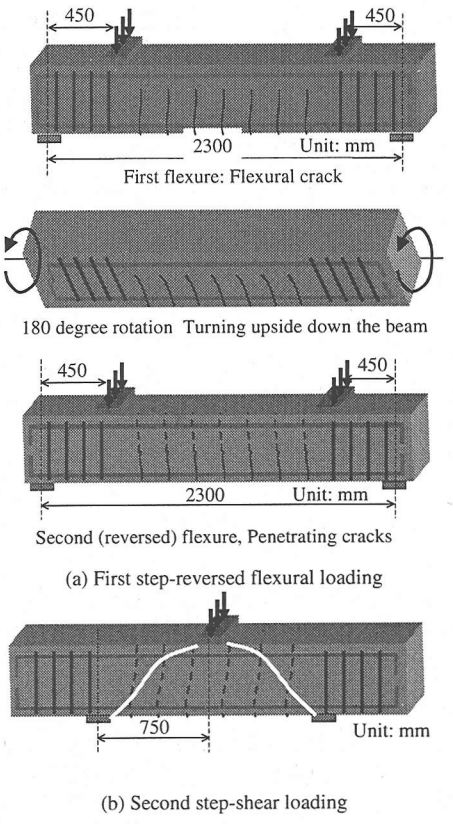

Fig.5 Experimental outline of shear test on pre-cracked beam[1)]

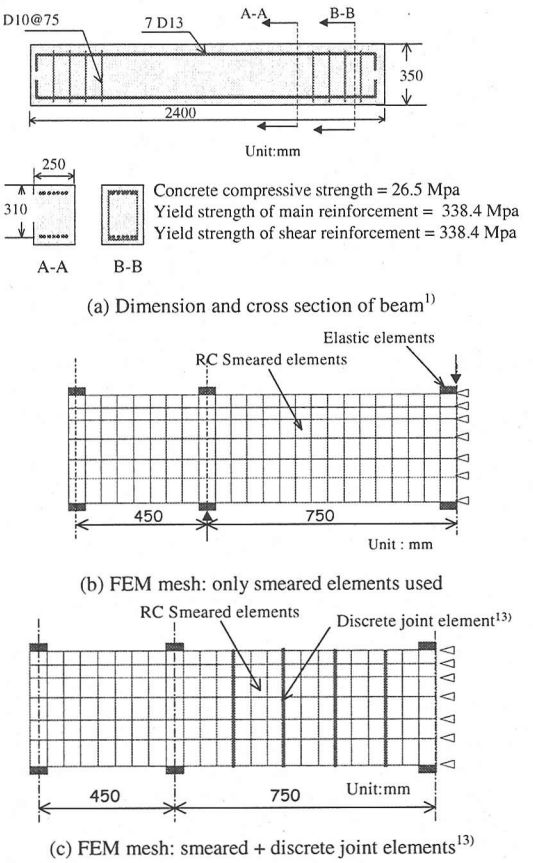

Fig.6 Dimensions, cross section, material properties and FEM mesh of pre-cracked beam problem

strength of concrete was 26.5 MPa. Tested yield strength of main bar was 338.4 MPa. The shear loading causes diagonal crack propagating across pre-crack planes.

The dimension and cross section of the beam are shown in **Fig.6a**. In the analysis, the authors consider two cases; one uses smeared elements only and the other uses both smeared and discrete joint elements to represent pre-cracks. The finite element meshes of these two cases are shown in **Fig.6b** and **Fig.6c**, respectively. These two analyses are referred as the smeared and smeared-discrete cases, respectively.

Load-displacement relationships under the shear loading (**Fig.7**) show that the behavior of pre-cracked beam significantly differs from the non pre-cracked one. Pre-cracked beam reaches considerably higher loading capacity, displacement ductility and energy consumption, but with much lower initial stiffness as compared to the non pre-cracked beam.

It is noted that numerical load-displacement curve is not smooth but shows the serrated pattern instead. In fact, experimental observation also demonstrated this characteristics, which is caused by the crack arrest and diversion mechanism[1)]. Once a diagonal crack is formed, load drops. However, since diagonal crack cannot propagate continuously across pre-crack planes, higher load can be resisted. The full smeared FEM shows some irregularity, since the applied larger element size represents few pre-cracks with blunt manner accompanying more cracking in the elements than the reality. The way to more realistically specify location of pre-cracking is to use smaller sized smeared elements that allow single cracking inside or joint interface ones. The latter way allows larger sizes of smeared elements covering the rest of analysis domain[8)].

The crack patterns during the initial stage of both cases are shown in **Fig.8**. Both smeared and smeared-discrete cases can predict Z-crack[1)] around each pre-crack similar to the experiment. In pre-cracked beams, Z-cracks are formed as a result of relative deformational contribution between pre-crack and diagonal crack[1)].

Failure crack patterns of both two cases are compared in **Fig.9**. FEM can capture well both main and secondary failure cracks for both smeared and smeared-discrete cases. The disconnected pattern of the main failure crack verifies that the analysis can reproduce the failure path through the independent

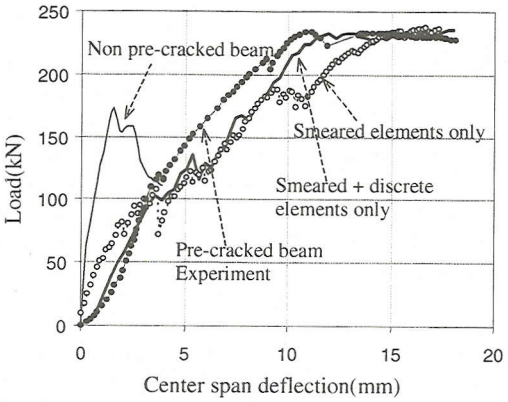

Fig.7 Comparison of numerical and experimental results

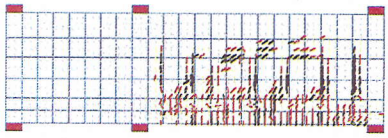

(a) Z-cracks captured in the smeared case

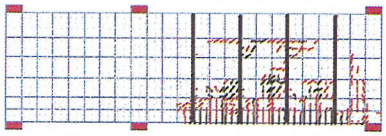

(b) Z-cracks captured in the smeared-discrete case

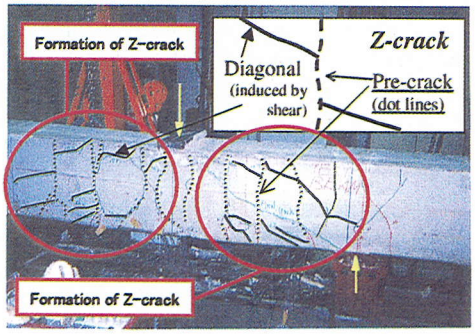

(c) Z-cracks in the experiment[1)]

Fig.8 Comparison of crack pattern during initial loading stage

formation of discontinuous diagonal cracks and subsequent combination of them.

One point is noted regarding the main failure crack pattern. When only smeared elements are used, the main failure crack is seen disconnected by the width of one element as shown in **Fig.9a**. However, when discrete joint elements are used, the width of discontinuity band is greatly reduced (**Fig.9b**). Hence, the combined use of smeared and discrete elements seems to give better results[8)].

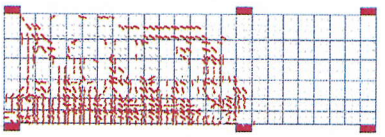

Secondary cracks captured by FEM

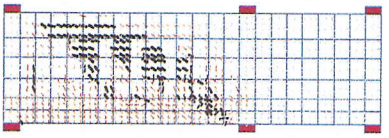

Main failure cracks captured by FEM

(a) Smeared case

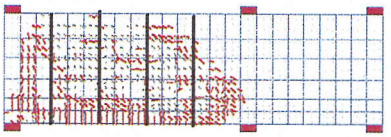

Secondary cracks captured by FEM

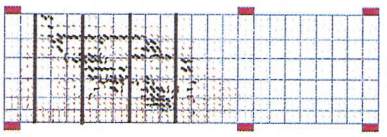

Main failure cracks captured by FEM

(b) Smeared + discrete case

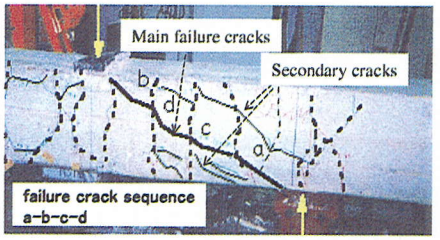

(c) Experimental failure crack pattern

Fig.9 Comparison of failure crack pattern[1)]

5. INFLUENCE OF LOADING PATHS ON RC BEHAVIOR

As mentioned before, the loading path is crucial for the RC behavior. Concrete is a highly path-dependent material recording its past events. Previous loading and environmental histories give the initial state of pre-cracks, pre-stress and pre-strain, i.e., path-dependency, into each RC element that constitutes the whole member. Different loading paths, though the same starting and ending points, may leave different path-dependency inside RC members and hence bring about different structural responses. In this section, the influence of loading path on the shear behavior of RC members will be investigated. The problem is defined in

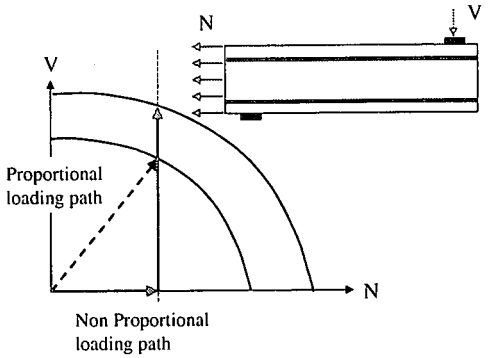

Fig.10 Definition of loading path in the analysis

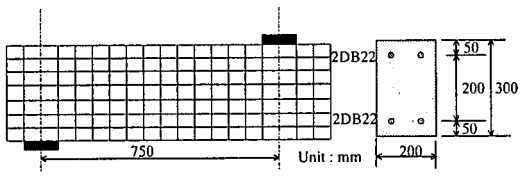

Fig.11 Finite element mesh of the problem

Fig.10. The RC beam is subjected to a coupled axial tension and shear loading.

In this study, two loading paths are examined. The first is the proportional loading path in which shear and axial tension are applied simultaneously to the RC beam. The analysis uses displacement control for applying shear and force control for applying axial tension. In each analysis, the step incremental displacement is kept constant for shear while the level of axial tension is varied. Through this analysis, the proportional loading path with varying ratio of shear and tension can be obtained.

For the non-proportional loading path, axial tension is applied first, maintained on the beam, and then shear is subsequently superimposed. The authors consider two cases, the first one is the initially un-cracked RC member and the second one is the initially pre-cracked RC member.

(1) Coupled axial tension – shear on initially un-cracked concrete: A discussion on JSCE code

This section discusses the effect of the coupled axial tension and shear on initially un-cracked concrete beam. The finite element mesh and the cross section of the target problem are shown in **Fig.11**. Due to symmetry, the analysis of half beam is sufficient. No transverse reinforcements are provided. Failure is designed to be the unstable propagation of diagonal shear crack before yielding of main reinforcements. The reinforcement ratio is 1.548%. Tensile strength of concrete is 1.62 MPa. The analysis for proportional loading path is conducted first. The result is shown in **Fig.12**. By varying the applied tension in each analysis, the beam reaches different shear capacity.

The general tendency is that the higher level of tension is applied, the lower shear capacity is reached. This is logical since the applied tension accelerates the formation of the diagonal crack and the first flexural crack also, which results in premature noticeable reduction in stiffness. However, the failure process is basically the same as in the beam without axial tension.

From the load-displacement relationship in the proportional loading analysis, the applied tensile stresses at the ultimate shear failure are obtained as followed: 0.00, 0.39, 0.71, 1.28, 1.84, 2.94, and 3.86 MPa. These tension values will be used in the analysis of non-proportional loading path.

The analysis of non-proportional loading path consists of two steps. In the first step, tension loading is applied. After that, it is kept in the memory and remained as the initial loading condition for the second analysis where shear loading is applied. It is noted that some of the above tensile stresses exceed the tensile strength of concrete, hence vertical cracks can occur. Thus, it is necessary to discuss the coupled effect of pre-crack and applied tension.

The relationship between load and displacement is shown in **Fig.13**. It is noticed that two distinct behaviors can be identified depending upon whether the applied tension exceeds tensile strength or not. As the level of applied tension increases, the reduction in shear capacity is observed but not in a smooth manner. When the applied tension exceeds the tensile strength, the analysis predicts higher capacity compared with the case in which the applied tension is lower than tensile strength. This indicates that there must be two failure envelopes for the non-proportional loading path.

First, the authors discuss the first category in which the applied tensile stress is less than tensile strength. Typical load-displacement curve shows a linearly elastic portion up to a certain extent depending on the level of applied tensile stress. As applied tensile stress increases, the first flexural crack is formed earlier and causes a noticeable decrease in stiffness. Moreover, the formation of the diagonal crack is also accelerated, which results in the premature shear failure. The failure process is basically the same as the proportional loading case. Applied tension that belongs to this group is 0.39 and 0.71 MPa.

Fig.14 illustrates the comparison between proportional and non-proportional loading analyses for the case in which the applied tension equals 0.71 MPa. The difference between two analyses is not significant except that the non-proportional loading

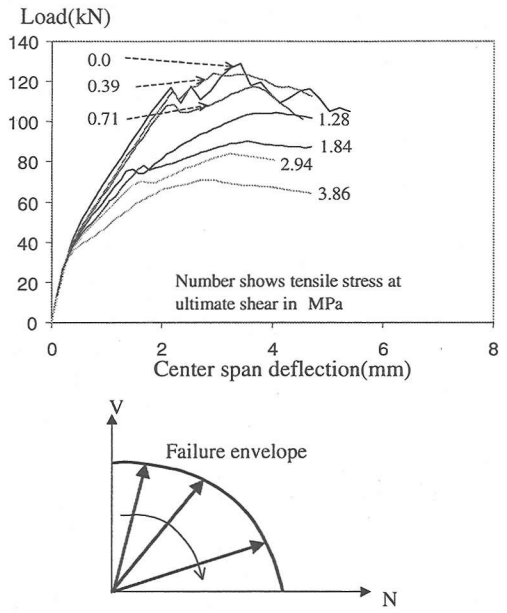

Fig.12 Load-displacement relationship for proportional loading analysis for initially un-cracked RC beam

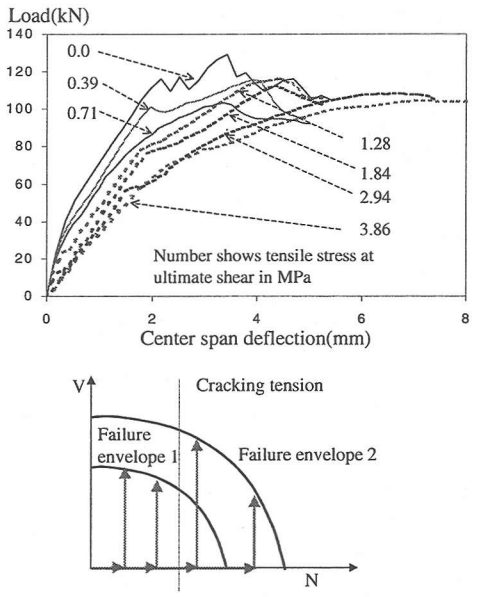

Fig.13 Load-displacement relationship for non-proportional loading path for initially un-cracked RC

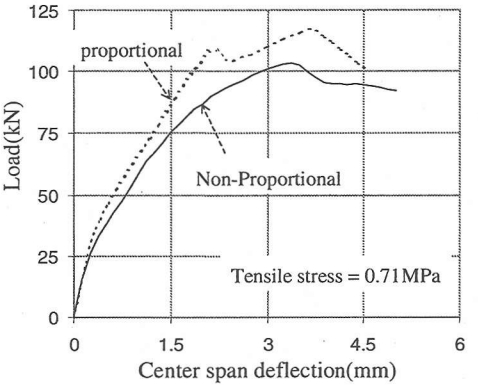

Fig.14 Comparison of proportional and non-proportional loading path analysis for tension = 0.71 MPa

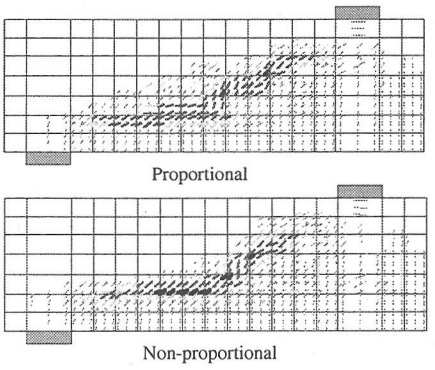

Fig.15 Comparison of crack pattern for proportional and non-proportional loading path
(applied tension < tensile strength)

case seems to predict slightly lower shear capacity. This is due to the fact that in the proportional loading path, the tension gradually increases from zero while in the non-proportional loading path, the full tension was applied to the beam from the beginning. Comparison of typical crack patterns between the two analyses is nearly the same as shown in **Fig.15**.

Next, the authors discuss the case in which the applied tension exceeds the tensile strength of concrete. In this case, tensile cracks due to applied tension are generated, which result in the pre-crack condition in RC beam. Due to these pre-cracks, under shear loading, no elastic portion appears on the load-displacement curve. In this case, the effect of crack interaction and the pre-tension mutually coexists. Pre-cracks tend to blunt the localization band of the diagonal crack[1] while pre-tension tends to accelerate the early formation of diagonal cracks.

Due to the predominant influence of pre-cracks, the non-proportional loading analysis in which the applied tension equals 1.84 MPa predicts higher capacity than the case in which the applied tension is 0.71MPa (**Fig.13**). Evidently, if applied tension is higher than concrete tensile strength, the effect of vertical cracks exists as well. The applied tensions that belong to this group are 1.84, 2.94 and 3.86 MPa. It is also noted that among these cases, the shear capacity is decreasing as the tension increases, which implies that the influence of applied tension is overcoming that of pre-cracks.

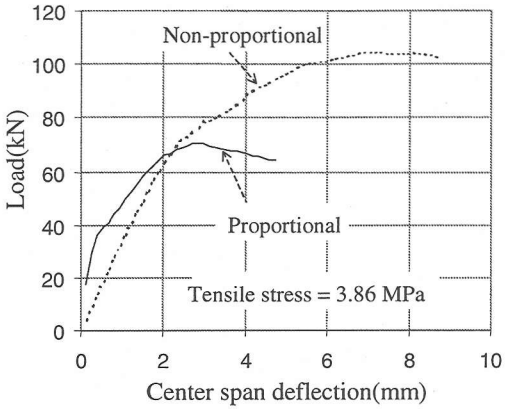

Fig.16 Comparison of proportional and non-proportional loading path analysis for tension = 3.86 MPa

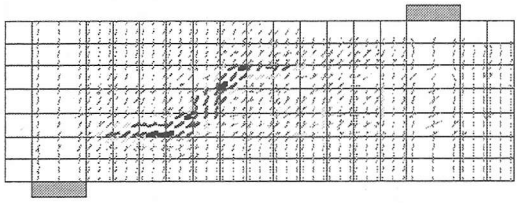

Fig.17 Failure crack pattern for proportional loading analysis, applied tension = 3.86 MPa

The comparison of load-displacement relationship between proportional and non-proportional loading paths for the case in which applied tension equals 3.86 MPa is shown in **Fig.16**. The non-proportional loading path predicts significantly higher shear capacity as explained. As for the failure process, the analysis in which applied tension equals 3.86 MPa is shown as an example. **Fig.17** shows the failure crack pattern of the proportional loading case. The analysis predicts the formation of diagonal crack in essentially the same way as in the non pre-cracked beam except that the diagonal crack is a little bit shifted to the left side of the beam. This diagonal crack, once developed, rapidly propagates upwards loading point and downwards support and forms the complete failure path. No crack interaction is shown in this case.

On the contrary, the non-proportional loading path shows a different result. The initial crack pattern in **Fig.18a** illustrates vertical pre-cracks resulted from the first axial tension loading. From the figure, it seems that vertical cracks do not penetrate the entire sections. This is due to the smeared element, which assumes that reinforcement is uniformly distributed in the element. Moreover, for the element that contains reinforcements, gradual stress release normal to crack is assumed due to bond effect. On the contrary, sharp stress

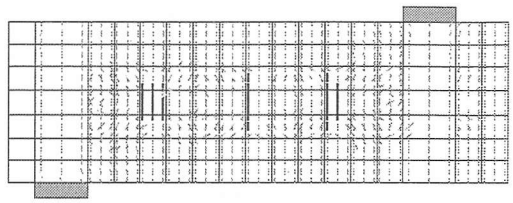

(a) Initial crack pattern

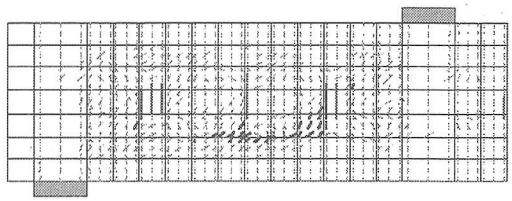

(b) Crack arrest phenomenon[1)]

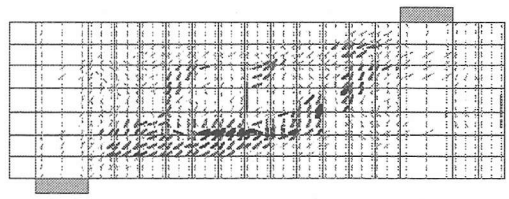

(c) Z-crack and discontinuity of the diagonal crack propagation

Fig.18 Typical failure crack pattern for non-proportional loading path: applied tension = 3.86 MPa

release is assumed for the element with no reinforcements. Therefore, cracks in the RC element containing no reinforcement are seen larger than those in the element containing reinforcements.

Under shear, the crack arrest phenomenon[1)] is shown in **Fig.18b**. The diagonal crack cannot propagate continuously across pre-crack planes. This results in the crack having a shape similar to alphabet Z and therefore referred as Z-crack (**Fig.18c**). Here, it is shown that the crack interaction exists, which results in a higher shear resistance compared with the proportional loading case.

The comparison of the proportional and non-proportional loading analyses for the case in which the applied tension equal 1.28 MPa is shown in **Fig.19**. Since the applied tension is close to tensile strength, i.e., f_t = 1.62 MPa, the non-proportional loading analysis predicts vertical cracks (point A in **Fig.19**), after a small portion of initial elasticity. **Fig.20** and **Fig.21** show crack patterns of proportional and non-proportional loading analyses, respectively for the case in which the applied tension equals 1.28 MPa. A more or less Z-crack pattern can be noticed in **Fig.21b**.

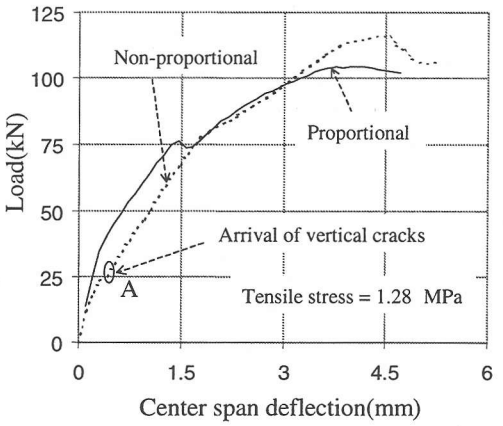

Fig.19 Comparison of proportional and non-proportional loading path analysis for tension = 1.28 MPa

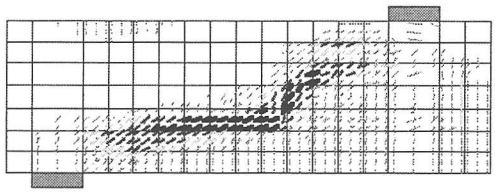

Fig.20 Failure crack pattern for proportional loading path, applied tension = 1.28 MPa

The comparison of failure envelope between the proportional and non-proportional loading analyses is shown in **Fig.22**. For the proportional loading path, the failure envelope can be described by a single curve. However, for the non-proportional loading path, two failure envelopes can be identified. The first envelope, designated as curve A, is for the case in which the imposed axial tensile stress is lower than tensile strength. Curve B represents the case in which the imposed tensile stress is near or higher than the tensile strength. The inclination of curve B is milder than curve A due to the influence of pre-cracks that blunt the localization of diagonal crack.

The JSCE design code[14] predicts the reduction in shear capacity of RC members subjected to axial tension by multiplying factor $\beta_n = 1+2M_0/M_u$ where M_0 is the counter flexural moment nullifying the tensile stress induced by axial force at tensile fiber of the member and M_u is flexural capacity. The JSCE prediction is plotted also in **Fig.22**. It is noted that JSCE prediction overestimates the analysis of proportional case and curve A of non-proportional one but underestimates the FEM result of curve B in the non-proportional loading path.

In literature, some experimental results of the shear test on RC beams subjected to axial tension have been reported[15)-17)], which showed no

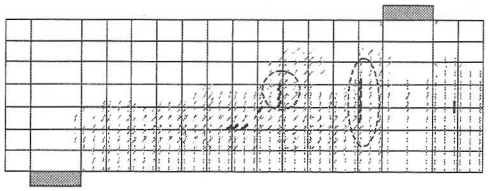

(a) Formation of vertical cracks corresponding to point A in **Fig.19**

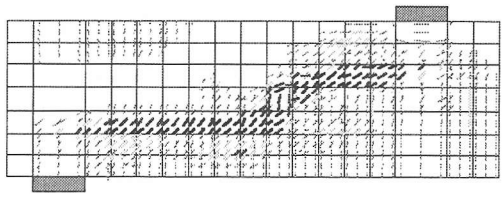

(b) Failure crack pattern

Fig.21 Typical failure crack pattern for non-proportional loading path: applied tension = 1.28 MPa

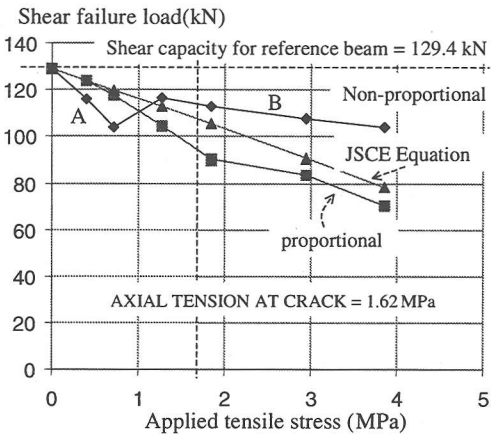

Fig.22 Comparison of failure envelope for proportional and non-proportional loading path

substantial degradation of shear capacity by applied tension. Even some researchers[15] reported the increase in shear capacity due to the axial tension. Therefore, axial tension, on one hand, decreases the shear capacity by accelerating the diagonal crack formation, on the other hand improves the shear capacity by generating pre-cracks which arrest the propagation of the formed diagonal crack. Generally, the increase or decrease of the shear capacity is possible depending on the relative contribution of two opposing effects resulted from the applied pre-tension. The relative effect depends on the width of pre-cracks and the level of applied tension.

Further analysis is conducted to show that FEM can capture the increase in shear capacity under the axial tension. For this purpose, the beam with the

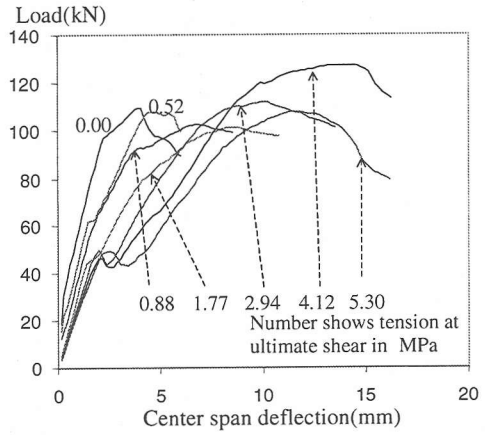

Fig.23 Load-displacement relationship

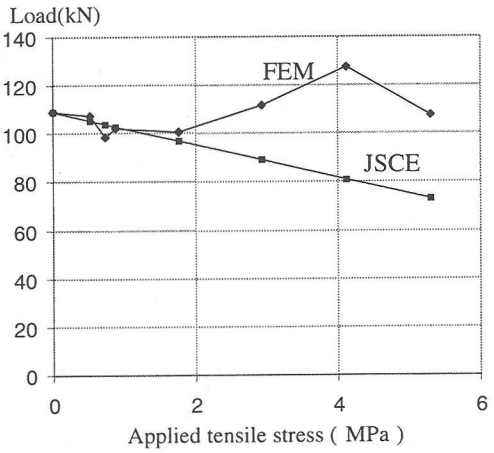

Fig.24 Failure envelope showing predominant influence of pre-cracks

same dimension and cross section as shown in **Fig.11** is used. Here, the reinforcement ratio and the tensile strength are assumed lower than the previous case so as to promote the influence of pre-cracks. The main reinforcement ratio and the tensile strength used in this analysis are 1.2% and 1.18 MPa, respectively.

The analysis results are shown in **Fig.23**. The failure envelopes predicted by JSCE and FEM are shown in **Fig.24**. It is seen that FEM captures the influence of pre-cracks in blunting the localization of diagonal cracks and hence leads to the increase in shear capacity even beyond that of the non pre-cracked beam.

The JSCE reduction factor is thought to account for the residual tensile stress in reinforcing bar resulted from the applied tension. In this way, the presence of tensile stress accelerates yielding and hence limiting the maximum load that can be applied on the member. In order to check this, the analysis is conducted and compared with the

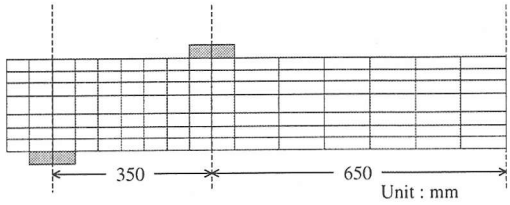

$\rho = 1.2\%$ Effective depth = 175 mm

Tensile strength = 3.24 MPa
compressive strength = 34.9 MPa
yield strength = 382.6 MPa
a/d = 2.0

(a) Tamura's experiment a/d = 2.0[17]

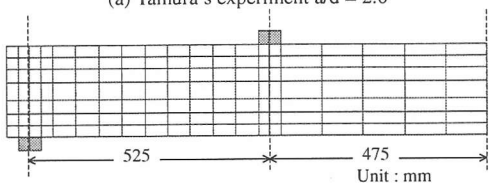

$\rho = 1.2\%$ Effective depth = 175 mm

Tensile strength = 3.43 MPa
compressive strength = 41.40 MPa
yield strength = 382.6 MPa
a/d = 3.0

(b) Tamura's experiment a/d = 3.0[17]

Fig.25 Simulation of Tamura's experiment

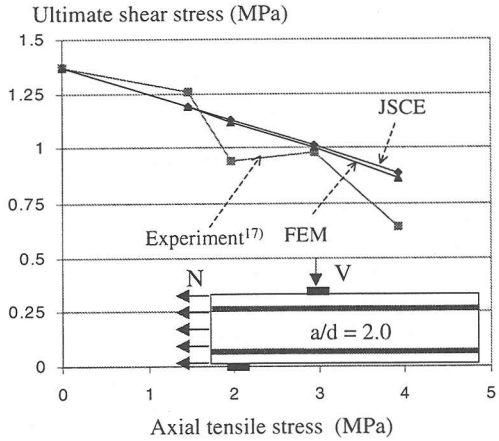

Fig.26 Simulation of Tamura's experiment (a/d = 2.0)

experimental results in which specimens fail in shear near or after yielding of main bars. Tamura's experiment[17] is used for this purpose. Two series of shear test on beam conducted by Tamura et al. are selected. The shear span to effective depth ratio is 2.0 and 3.0, respectively. Finite element mesh and material properties of these two cases are shown in **Fig.25**.

The comparison of experimental result, FEM and JSCE predictions is shown in **Fig.26** and **Fig.27** for a/d equals 2.0 and 3.0, respectively. Experimental results can be fairly predicted. The tendency that shear capacity decreases as the applied tension increases can be reproduced. From the failure

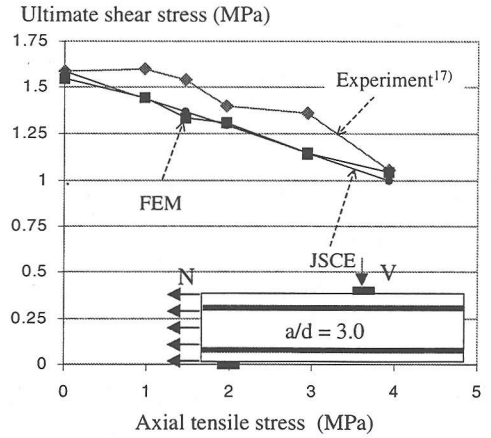

Fig.27 Simulation of Tamura's experiment (a/d = 3.0)

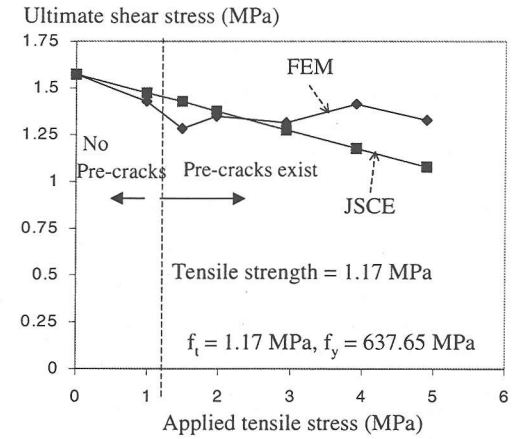

Fig.30 Failure envelope for beam (a/d = 3.0) with predominant influence of pre-cracks

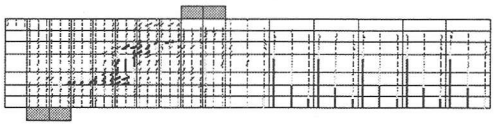

Fig.28 Numerical crack pattern for a/d = 2.0 (tensile stress = 1.96 MPa)

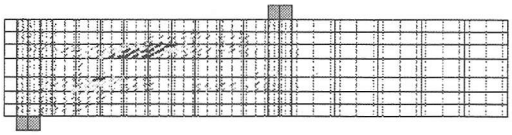

(a) Initial crack pattern: Z-cracks

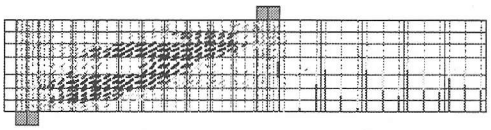

(b) Failure crack pattern

Fig.29 Numerical crack pattern for a/d = 3.0 (tensile stress = 1.96 MPa)

envelope, it is noticed that FEM closely matches the JSCE prediction. All analyses predict shear failure after yielding. As discussed before, the effect of axial tension here is to give the initial stress to the main reinforcement and hence accelerate its yielding. Typical numerical failure crack patterns are shown in **Fig.28** and **Fig.29** for a/d = 2.0 and 3.0, respectively. The crack patterns show both flexural and shear cracks.

From the above analyses, it is seen that the JSCE reduction factor is applicable for the problem in which shear failure takes place near or after yielding of main bars. This is due to the effect of initial stress in the reinforcing bars, i.e., from axial tension, which reduces the yielding moment of the beam. Generally, three main effects may be identified due to the applied axial tension, namely, (1) initial stress in reinforcing bar reduces the yielding moment; (2) axial tensile stress tends to accelerate the arrival of diagonal cracks; and (3) pre-cracks from axial tensile stress tend to alleviate the localization of diagonal cracks.

JSCE reduction factor seems to consider only the first effect. The second and the third effects are not explicitly treated in the code. If shear and axial tension are concurrently applied as in the proportional loading path, no pre-cracks are created, thus the acceleration of the diagonal crack becomes prominent. In this case, JSCE tends to overestimate the FEM result. However, in the non-proportional loading path, if axial tension is higher than tensile strength, the influence of pre-cracks exists and counteracts the diagonal crack acceleration. In this case, JSCE tends to give conservative results.

A further analysis is conducted to verify the above understanding. The mesh of Tamura's experiment for the case in which a/d equals 3.0 (**Fig.25b**) is used. However, the yielding strength of main bars used is 637.65 MPa, about 1.66 times that in the Tamura's experiment so that shear failure occurs long before yielding of main bars. Tensile strength is assumed smaller also, i.e., f_t = 1.17 MPa compared with 3.43 MPa in the previous analysis. In this case, the influence of pre-cracks is dominant. Comparison of failure envelopes predicted by FEM and by JSCE is shown in **Fig.30**. It is shown that a certain difference exists between FEM and JSCE predictions. In the range where applied axial tensile stress is less than tensile strength, JSCE tends to overestimate the shear capacity. However, it gives conservative results when applied tensile stress is higher than tensile strength.

Regarding the effect of shear span to effective depth ratio, i.e., a/d, Tamura et al.[17] reported that for smaller a/d, shear capacity drops more rapidly

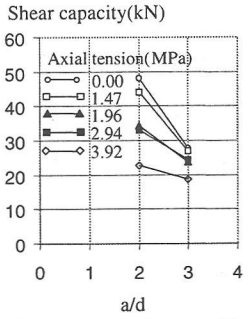

(a) Tamura's experiment[17]

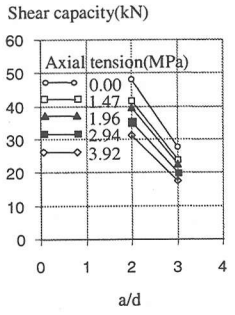

(b) JSCE prediction

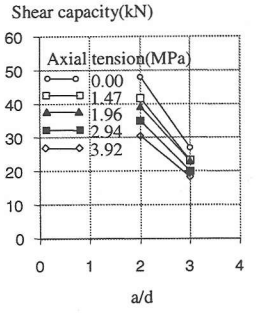

(c) FEM

Fig.31 Influence of a/d on the decrease in shear capacity (comparison with Tamura 's experiment[17] **Fig.25**)

as applied tension increases. The drop of shear capacity is shown comparatively for Tamura's experiment, JSCE and FEM predictions in **Fig.31**. It is seen that the experiment shows stronger effect of a/d ratio than the JSCE and FEM predictions. The effect of various factors such as a/d ratio, yield strength and ratio of main reinforcements and tensile strength of concrete on the shear capacity of RC beam has been investigated in more detail by An et al[9].

(2) Coupled axial tension – shear on pre-cracked RC members

In the previous analysis, the main target of investigation is the initially un-cracked RC member. Now, the authors discuss the initially pre-cracked RC member. Finite element mesh for this analysis is the same as the previous case (**Fig.11**). The only difference from the previous analysis is the introduction of pre-cracks into the beam. For this purpose, the beam is applied axial tension first. Load-displacement relationship under this tension is shown in **Fig.32a**. The initial crack pattern is shown in **Fig.32b**.

Similar to the previous case, the analysis for proportional loading path is conducted first. In this case, axial tension is simultaneously applied with the shear load. The load-displacement for each applied tension is shown in **Fig.33**. As shown in the

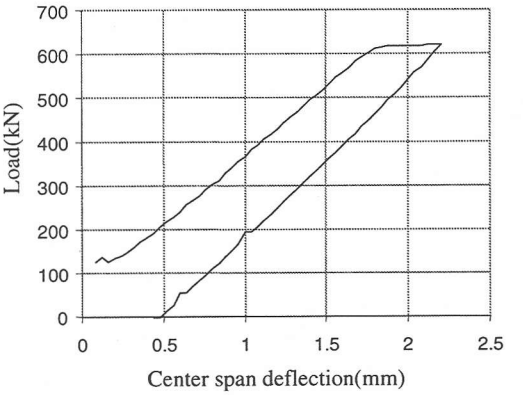

(a) Load-displacement relationship for axial tension

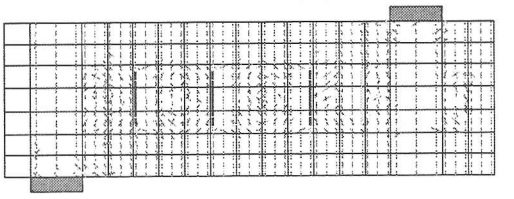

(b) Initial vertical pre-cracked condition

Fig.32 Applied axial tension to introduce pre-cracks

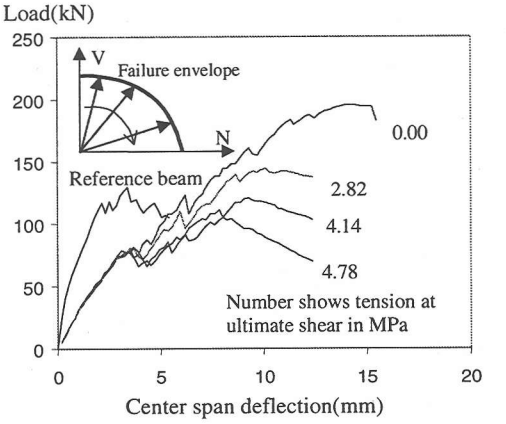

Fig.33 Load-displacement relationship for proportional loading analysis for initially pre-cracked RC

figure, shear capacity decreases as the applied tension increases. From these load-displacement curves, the level of applied tensile stresses at the ultimate shear failure are obtained as follows; 0.00, 2.82, 4.14, 4.78 MPa. The typical failure process is described in **Fig.34** for the case in which the applied tension equals 4.78 MPa. The formation of Z-cracks[1] is predicted as shown in **Fig.34a**. The failure crack pattern in **Fig.34b** shows the formation of discontinuous diagonal cracks linking loading point to support.

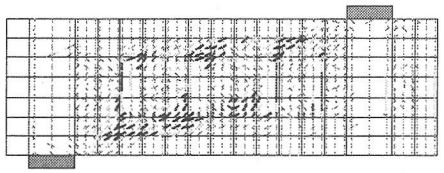

(a) Initial Z-crack pattern

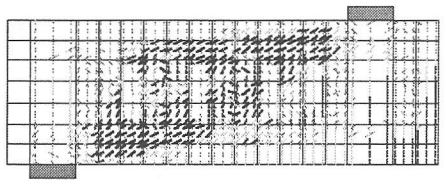

(b) Failure crack pattern

Fig.34 Crack pattern for proportional loading path, applied tension = 4.78 MPa

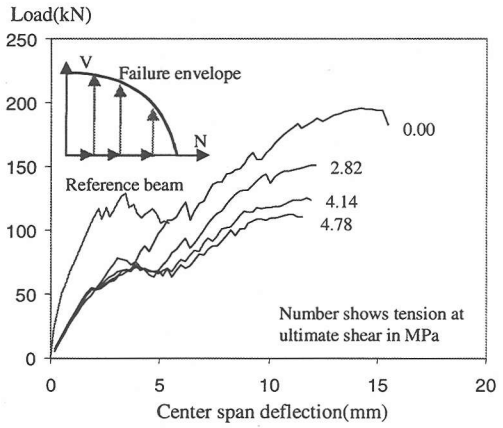

Fig.35 Load-displacement relationship for the non-proportional loading analysis for initially pre-cracked RC

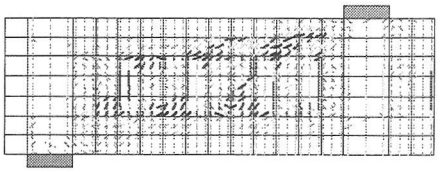

(a) Initial Z-crack pattern

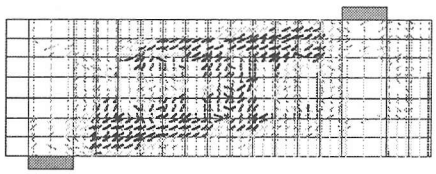

(b) Failure crack pattern

Fig.36 Crack pattern for the non-proportional loading path, applied tension = 4.78 MPa

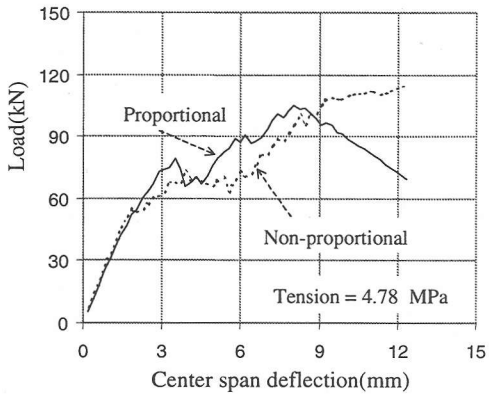

Fig.37 Comparison of proportional and non-proportional loading path analysis for tension = 4.78 MPa, pre-cracked beam

Next, the analysis for the non-proportional loading path is conducted. First, the above tensile stresses are applied to the beam and remained on it throughout the subsequent shear loading. Load-displacement relationships are shown in **Fig.35**. As shown in the figure, shear capacity decreases continuously as the applied tension increases. Unlike the analysis of initially un-cracked members, the analysis here predicts a single failure envelope. The typical failure process is basically similar to the proportional loading analysis. Z-crack and discontinuous pattern of failure diagonal crack are shown respectively in **Fig.36a** and **Fig.36b** for the case in which the applied tension equals 4.78 MPa.

Comparison of load-displacement relationship between the proportional and non-proportional loading paths is shown in **Fig.37** for applied tension equals 4.78 MPa. No significant difference between the two analyses is noticed. The proportional loading analysis gives slightly higher stiffness before peak but predicts slightly lower shear capacity. This is reasonable since in the proportional loading analysis, tension is gradually increasing from zero, but it remains fixed at certain values from the beginning in the non-proportional loading path. Therefore, during the initial loading stage, the applied tension in the proportional loading analysis is lower than the non-proportional one. At the peak, the applied tension between two cases is the same. After the peak, the applied tension in the proportional loading exceeds the corresponding non-proportional one, which explains why the proportional loading analysis predicts slightly lower capacity than the non-proportional counterpart.

Failure envelopes of the proportional and non-proportional paths are shown in **Fig.38**. The failure envelopes of the proportional and non-proportional loading paths for initially un-cracked and pre-

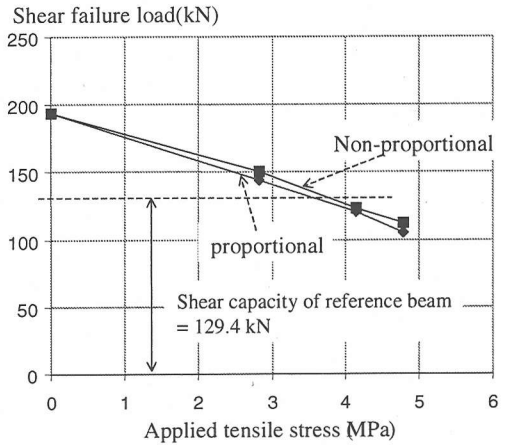

Fig.38 Comparison of failure envelope for proportional and non-proportional loading path: pre-cracked beam

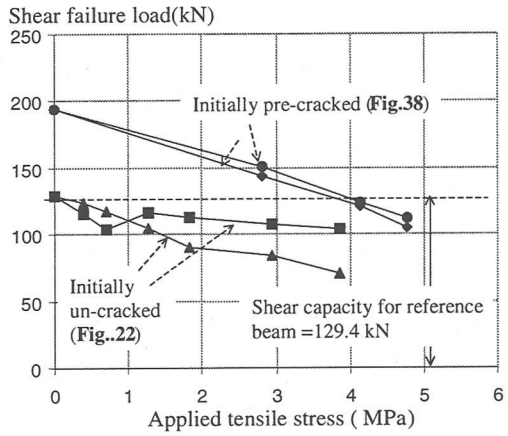

Fig.39 Comparison of failure envelope for proportional and non-proportional loading path: un-cracked and pre-cracked beam

cracked beams are plotted together in **Fig.39**. From this figure, the effect of pre-crack and pre-tension on shear capacity is identified. Pre-cracks tend to elevate the loading capacity while the applied tension tends to decrease it.

Finally, the authors conduct the analysis of the beam with very large pre-cracks together with very high tension. In this case, shear transfer along pre-cracks is substantially decreased and thus disables the activation of diagonal cracks. The introduction of pre-cracks in the RC beam is implemented by axial tension as before, but with much higher value compared to the previous analysis. The load-displacement under axial tension and the initial crack pattern are shown in **Fig.40**. After that, tensile stresses of 0.49, 2.45, and 4.90 MPa are applied to the beam and followed by the application of shear loading. The relationships between load and displacement are given in **Fig.41**. The reference

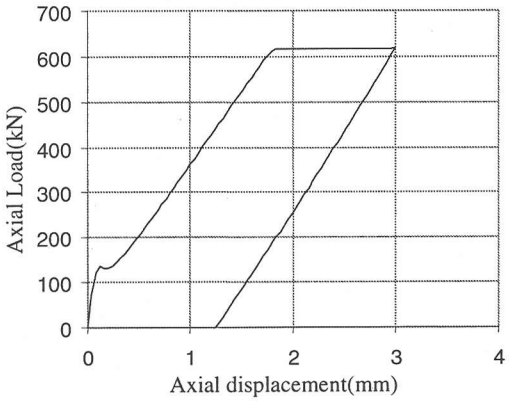

(a) Load-displacement relationship for axial tension

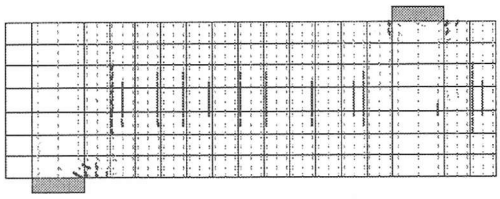

(b) Initial vertical pre-cracked condition

Fig.40 Applied axial tension to introduce pre-cracks

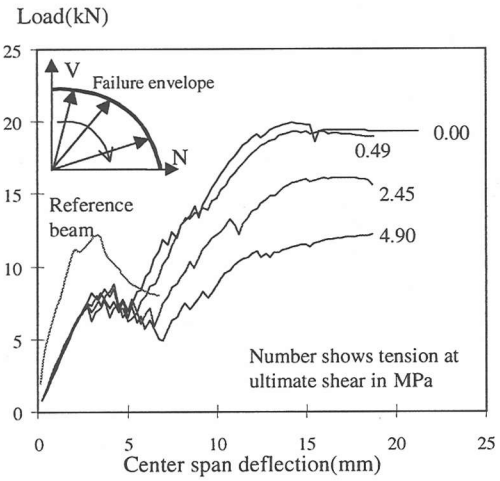

Fig.41 Load-displacement relationship for the non-proportional loading analysis for large pre-cracked RC

beam is the one with neither applied pre-tension nor pre-cracks. The similar tendency to the previous case is obtained, that is, shear capacity decreases as tension increases.

The crack pattern for the case in which applied tension equals 4.9 MPa is shown in **Fig.42a**. The analytical crack pattern shows no diagonal cracks around the web portion of the beam. Here, the behavior of the beam is governed by the activation of pre-tensile stress and pre-cracks. Since the width

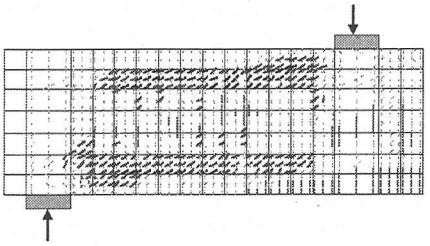

(a) Crack pattern and failure strain distribution

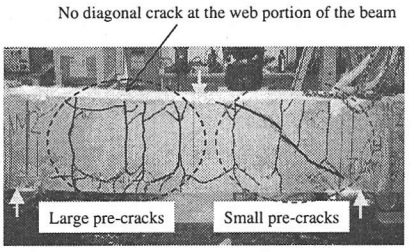

(b) Experimental manifestation

Fig.42 Numerical and experimental crack pattern very low shear modulus at the pre-crack interface

of pre-cracks is large, the shear transfer due to aggregate interlock is significantly reduced, thus, no diagonal cracks can penetrate the web portion. This analysis shows the effect of pre-cracks.

The fact that no diagonal cracks penetrate the web portion in the beam with large pre-cracks could also be obtained in the experiment as shown in **Fig.42b**. As shown in the figure, the left side of the beam is totally dominated by pre-cracks. The beam was failed by shear in the right side, which had considerably smaller pre-cracks.

6. CONCLUSIONS

The paper addresses the numerical analysis of RC members subjected to non-proportional loading path and pre-cracked conditions. Fixed crack approach is employed since it explicitly and independently treats the normal and shear actions, which is the key for the simulation of shear anisotropy at the pre-crack interface.

The behavior of RC member subjected to coupled axial tension and shear is investigated. The simultaneous influence of pre-stress and pre-crack is numerically discussed. Depending on the loading paths, axial tension differently affects the shear capacity of the RC beam. For proportional loading path in which shear is applied concurrently with axial tension, the latter will accelerate the formation of the diagonal crack, thus results in the premature shear failure.

For the non-proportional loading path in which axial tension is applied first, maintained on the beam and followed by shear, the effect of axial tension is various. Three main influences can be identified as follows; (1) the initial stress in the reinforcement causes early yielding; (2) axial tensile stress accelerates the formation of diagonal crack; and (3) pre-cracks caused by axial tension blunt the localization of diagonal crack. It is noted that the second and the third factors give contradictory effect despite the fact that they are caused by the same axial tension. Depending on the relative effects of the above factors, the shear behavior of RC beam subjected to axial tension is various. The increase or decrease in capacity has been experimentally demonstrated. The JSCE design code predicts only the reduction in shear capacity corresponding to the first factor, without the explicit consideration of the second and the third ones.

Finally, the significance of shear transfer along pre-crack interface is demonstrated. The behavior of pre-cracked beam is various. It can be totally dominated by the diagonal crack only or pre-crack only or a mixed behavior between pre-crack and diagonal crack. The latter reflects the relative contribution of pre-crack and diagonal crack deformation. Shear transfer due to aggregate interlock is indispensable to capture the shear anisotropy at pre-crack interface.

ACKNOWLEDGEMENT: The authors would like to express their gratitude towards the Grant-in-aid for scientific research no. 12450174 in providing financial supports for carrying out the research.

REFERENCES

1) Pimanmas, A. and Maekawa, K.: Influence of pre-crack on RC behavior in shear, *Accepted for publication in J.Mat.Conc.Strcut.Pavements, JSCE.*
2) Pimanmas, A. and Maekawa, K.: Finite element analysis and behavior of pre-cracked reinforced concrete member in shear, *Accepted for publication in Magazine of concrete research.*
3) Pimanmas, A. and Maekawa, K.: Multi-directional fixed crack approach for highly anisotropic shear behavior in pre-cracked RC members, *Accepted for publication in J.Mat.Conc.Strcut.Pavements, JSCE.*
4) Pimanmas, A. and Maekawa, K: Control of crack localization and formation of failure path in RC members containing artificial crack device, *Accepted for publication in J.Mat.Conc.Struct.Pavements, JSCE.*
5) Mabrouk, R., Ishida, T. and Maekawa, K.: Solidification model of hardening concrete composite for predicting creep and shrinkage of concrete, *Proc. of JCI*, Vol.20, pp.691-696, 1998.

6) Fukuura, N. and Maekawa, K.: Re-formulation of spatially averaged RC constitutive model with quasi-orthogonal bi-directional cracking, *Proc. of JSCE*, Vol. 45, pp. 157-176, 1999. (in Japanese)
7) Fukuura, N. and Maekawa, K.: Spatially averaged constitutive law for RC in-plane elements with non-orthogonal cracking as far as 4-way directions, *Proceeding of JSCE*, Vol.45, pp. 177-195, 1999. (in Japanese)
8) Okamura, H. and Maekawa, K.: *Nonlinear analysis and constitutive models of reinforced concrete*, Gihodo-Shuppan Co. Tokyo, 1991.
9) An, X., Maekawa, K. and Okamura, H.: Numerical simulation of size effect in shear strength of RC beams, *J. Materials Conc. Struct., Pavements, JSCE*, Vol.35, No. 564, pp.297-316, 1997.
10) Li, B., Maekawa, K. and Okamura, H.: Contact density model for stress transfer across cracks in concrete, *J. Faculty of Eng. Univ. of Tokyo(B)*, Vol.40, pp.9-52, 1989.
11) Salem, H. and Maekawa, K.: Spatially averaged tensile mechanics for cracked concrete and reinforcement under highly inelastic range, *J. Mater. Conc. Struct. Pavement*, JSCE, pp. 277-293, 1999.
12) Hauke, B. and Maekawa, K.: Three-dimensional modelling of reinforced concrete with multi-directional cracking, *J.Mat.,Conc.Struct.,Pavements, JSCE*, Vol.45, pp.349-368, 1999.
13) Mishima, T. and Maekawa, K.: Development of RC discrete crack model under reversed cyclic loads and verification of its applicable range, *Concrete library of JSCE*, No.20, 1992.
14) Standard Specification for design and construction of concrete structures –1986 part 1[design], JSCE
15) Yamada, K. and Kiyomiya, O.: Shear resistance of reinforced concrete beams with initial penetrating cracks, *JCI*, Vol.17, No.2, pp. 791-796, 1995. (In Japanese)
16) Tamura, T., Shigematsu, T. and Nakashiki, K.: About the increase in shear capacity of RC beam under axial tension, *Proc. of the 54th JSCE annual convention*, pp.608-609, 1999. (In Japanese)
17) Tamura, T., Shigematsu, T., Hara, S. and Nakano, S., Experimental analysis of shear strength of reinforced concrete beams subjected to axial tension, *Concrete Research and Technology*, JCI, Vol.2, No.2, 1991.

(Received June 8, 2000)

軸引張力とせん断組み合わせ経路を受けるRC部材のせん断破壊

ピマンマス　アモン・前川　宏一

本研究は，ＲＣ部材の挙動に及ぼす載荷経路の影響について検討するものであり，軸引張力とせん断力の経路とせん断耐力の関係に着目したものである．軸引張力は，1) 鋼材の降伏を早めること，2) 斜めひび割れの発生を加速することの他に，3) 部材軸方向にひび割れを発生させて，斜めせん断ひび割れの進展を遅らせる効果もある．これらの効果の組み合わせで，軸引張力が部材のせん断耐力を低下させる場合も，向上させるもあることを示した．実験結果と解析結果との比較検討を行い，設計示方書では部材せん断耐力を低下させる要素のみを耐力算定式で考慮し，安全側の評価を与えていることを確認した．